MINERALOGICAL MAGAZINE, JUNE 1974, VOL. 39, PP. 672–683.

Compositional variation within staurolite crystals from the Ardara aureole, Co. Donegal, Ireland

J. A. T. SMELLIE

Department of Geology, Queen's University, Belfast

SUMMARY. Staurolite crystals from the aureole of the Ardara pluton have been analysed using the electron microprobe. Compositional variations of TiO_2, MnO, and MgO take the form of irregular zoning, differences across sector twin boundaries, and variable marginal compositions, and can be attributed mostly to disequilibrium and localized diffusion.

FEW analytical data exist for staurolite, in comparison with other metamorphic minerals such as garnet. However, using the microprobe, Hollister and Bence (1967) working with relatively inclusion-free specimens from the Kwoiek Area, British Columbia, established compositional zoning across staurolite in addition to compositional irregularities across sectoral twin boundaries.

The staurolites studied from Ardara were collected from a single formation, the Gleengort (Clooney) Pelitic Schists, which occur in the thermal aureole surrounding the Ardara Pluton, Co. Donegal (fig. 1). Eighteen staurolite crystals, including several that showed sector twinning, were analysed to establish the presence or absence of zoning, which might help to explain nucleation and growth.

Petrography

The petrography of the Ardara aureole is well documented (Akaad, 1956*a*, *b*; Pitcher and Sinha, 1958; Pitcher and Read, 1963; Naggar and Atherton, 1970; and Smellie, 1972, *b*). Thermal metamorphism, which resulted from the emplacement of the Ardara Pluton, was superimposed on the pre-existing regional metamorphic rocks dominated by chlorite–garnet–muscovite schists. This produced, in order of decreasing distance from the contact, biotite, garnet, staurolite, andalusite, sillimanite, and cordierite (Smellie, 1972 *b*). Generally the thermal garnets occur as small euhedral crystals (up to 0·25 mm in diameter) containing a dark core of included graphite and cross-cutting the pre-thermal foliation (fig. 2*a*). In some cases, especially in the mica-rich bands, these thermal garnets show some alteration to biotite, forming in places atoll garnet rims, with the garnet core mainly replaced by biotite. The regional, pre-thermal garnets still existing tend to be larger (up to 0·80 mm in diameter) exhibit syntectonic textures, and are usually in an advanced state of alteration forming, eventually, biotite pseudomorphs.

The appearance and gradual disappearance of staurolite enables a staurolite-dominant sub-zone to be distinguished within the staurolite–andalusite zone (fig. 1)

© Copyright the Mineralogical Society.

(Smellie, 1972 *b*). It first appears about 1000 metres from the igneous contact, growing in muscovite-rich bands and showing no obvious relationship with the thermal garnet. The crystals are small (approx. 0·4 mm in length), anhedral, and fringed by small flakes of biotite.

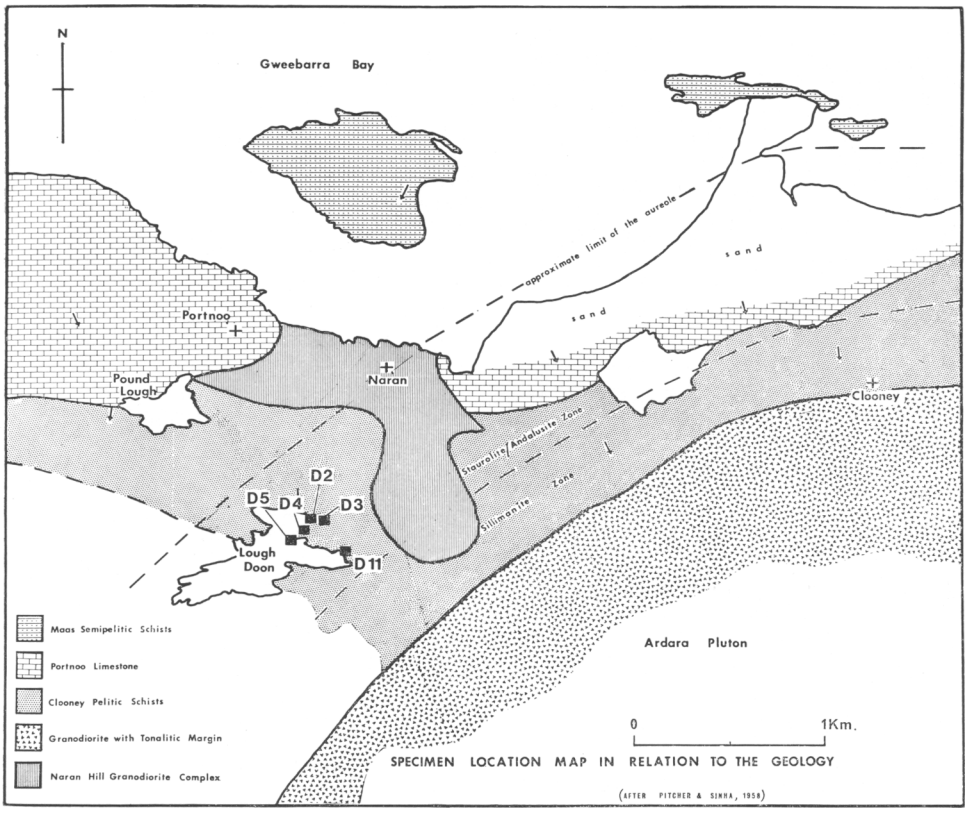

FIG. 1. The north-western part of the aureole, Ardara Pluton, Co. Donegal, showing the location of the specimens in relation to the geology. (After Pitcher and Sinha, 1958).

As there is negligible biotite in the mica-rich bands away from the staurolite, the presence of small amounts of biotite near the staurolite indicates the reaction: chlorite+muscovite → staurolite+biotite+quartz+H_2O. Nearer to the contact, extensive biotite growth, commonly parallel to the schistosity, tends to obliterate such textural relationships, but the close association of staurolite with mica-rich bands indicates that this reaction is widespread within the staurolite-dominant sub-zone.

With increasing temperature, a later generation of staurolite has developed partly from biotite, which, by this stage, has replaced chlorite in the original schistosity. Such staurolite crystals tend to be smaller (0·05 to 0·50 mm in length) than the earlier variety and relatively inclusion-free. These may have resulted from the reaction:

biotite$_1$+muscovite → biotite$_2$+staurolite+quartz+H_2O. During this later growth episode, staurolite forms within the biotite pseudomorphs after regional garnet (fig. 2*c*), and partial pseudomorphs after thermal garnet. Only in exceptional cases does the staurolite occupy almost the complete volume of the pseudomorph and sporadically include a remnant regional garnet. Where staurolite is associated with the former

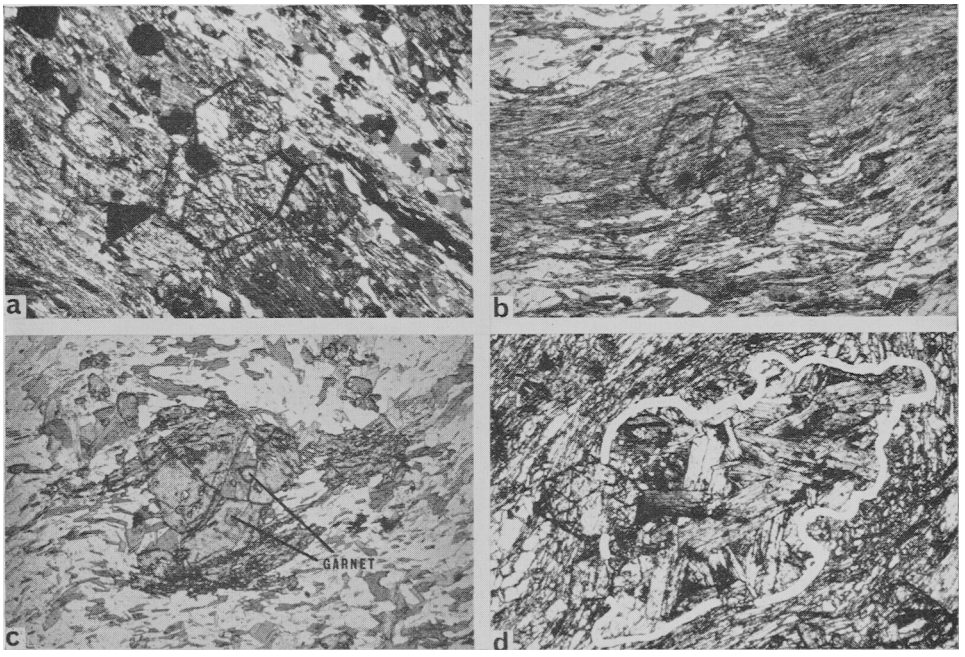

FIG. 2. *a*: Idiomorphic staurolite crystals fringed with dark graphite formed in mica-rich bands and almost completely enclosing a thermal garnet (black). Other thermal garnets are shown cross-cutting the bands. Note the small biotite embayments in two of the garnets. Crossed nicols; ×16 diameters. *b*: Staurolite, fringed with dark graphite, growing mainly in the pre-thermal mica-rich band and preserving concordant inclusion trails. Plane polarized light; ×16 diameters. *c*: Staurolite forming within a biotite pseudomorph after regional garnet and enclosing two remnant regional garnet fragments. Note the development of staurolite in the mica-rich bands wrapped around the pseudomorph in a syntectonic manner. Plane polarized light; ×12·5 diameters. *d*: Small euhedral staurolite growing partly in the mica-rich bands and partly within a biotite pseudomorph after regional garnet (denoted by the white line). Plane polarized light; ×16 diameters.

pseudomorphs it usually occurs either in the mica-rich bands (according to the first reaction), which wrap around the pre-existing syntectonic regional garnet (fig. 2*c*), or penetrate slightly into the pseudomorphs (fig. 2*d*). The close association of garnet and staurolite in these cases suggest the reaction: muscovite+chlorite+garnet → staurolite+biotite+quartz+H_2O. However, the microprobe analyses indicate that the staurolite formed from the biotite (i.e. the biotite that has partly replaced the garnet), with the staurolite eventually enveloping the garnet fragments.

Staurolite is best developed about 700 to 900 m from the contact, where the crystals

are up to 1·0 mm in length. The degree of idiomorphism is related to the occurrence of staurolite in mica-rich bands, for example, where the approximate content of the band is 45 % muscovite+chlorite, 40 % quartz+feldspar, and 10 % biotite, the staurolite growth is prolific and included garnets are common (fig. 2*a*). The staurolite is spongy in appearance and slightly pleochroic; the relict schistosity and crenulation cleavages can be traced through the staurolite poikiloblasts by concordant sigmoidal inclusions mostly of quartz, plus small amounts of mica, magnetite, and graphite (fig. 2*b*). Sector twinning is quite common.

TABLE I. *Analyses of two lithological bands (A and B) and associated staurolites from the same specimen (D_3)*

	A	SA	B	SB	Modes§		
SiO_2	64·0	n.d.	53·7	n.d.	A		B
TiO_2	0·61	0·42	1·13	0·55	Q/F.	50·2	19·3
Al_2O_3	16·4	53·8	26·0	53·4	M.	9·8	65·1
Fe_2O_3	3·2	14·0*	2·5	13·8*	Bi.	34·3	4·7
FeO	4·0†	n.d.	2·8†	n.d.	St.	4·3	9·4
MnO	0·03	0·34	0·04	0·36	Acc.	1·4	1·5
MgO	2·2	1·5	1·9	1·5			
CaO	0·84	n.d.	0·99	n.d.			
Na_2O	n.d.	n.d.	n.d.	n.d.			
K_2O	3·0‡	n.d.	4·4	n.d.			
H_2O	n.d.	n.d.	n.d.	n.d.			
Total	94·28	70·06	93·46	69·61	100·0		100·0

* Total iron as Fe_2O_3.
† Classical wet chemical method.
‡ Rapid wet chemical method.
§ Q/F—Quartz and feldspar; M—Muscovite; Bi.—Biotite; St.—Staurolite; Acc.—Accessories.
A,B: Rock analyses, by X-ray fluorescence.
SA, SB: Staurolites from A and B respectively, electron-probe analyses.

The distribution of staurolite within the aureole is more restricted than that of garnet and biotite. This is also quite common in other areas and previous workers have emphasized a dependence of its occurrence on the host rock composition (Williamson, 1953; Ellitsgaard-Rasmussen, 1954; Atherton, 1965). Juurinen (1956), however, suggests a much smaller dependence on host rock composition. Williamson (1953) and Atherton (1965) stress a low MgO value and a Fe_2O_3/Al_2O_3 ratio of around 0·40 in staurolite-bearing rocks. Data from two adjacent bands, both containing staurolite, are compared in Table I. Although the bands vary considerably in composition, typical analyses of staurolites from each band indicate little variation.

Analytical procedure

Microprobe analyses were carried out using a Cambridge Instrument Company Geoscan at 20 to 25 KV, 0·045 to 0·065 microamperes, and a beam diameter of 2 to

4 μm. Homogeneous glass standards (Smellie, 1972 *a*) of equivalent total mass absorption coefficients to staurolite were used. The raw data were converted to compositional data simply by calculating the ratio of unknown to standard minus background. The only other correction necessary was a small one for the atomic number. The results are reproducible to within 2 % (counting error of the probe); the accuracy of determining individual oxides ranges from 2 to 4 % depending on the percentage of the oxide present, and sums for total analysis are 100±2 % (Smellie, 1972 *b*).

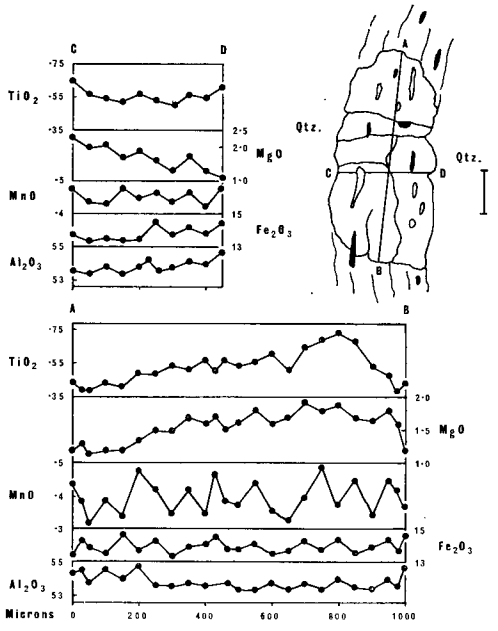

FIG. 3. Microprobe traces across a staurolite crystal formed along a narrow mica-rich band bordered by quartz or a quartz-rich matrix. Black areas are ore and clear inclusions are quartz. Scale bars are 200 μm and all elements are expressed as percentage weight of the oxides. Analyses not shown can be considered uniform across the crystal.

Results

Examples were analysed of staurolite resulting from growth in the pre-existing mica-rich matrix, growth within the regional garnet pseudomorphs, and growth from biotite formed by the partial replacements of some thermal garnets. In addition analysis of the compositional variation across sector twin boundaries was carried out.

Staurolite formed in the pre-existing matrix. Specimen D_2 (fig. 1) contains staurolite that has grown along mica-rich bands, preserving a relict schistosity as concordant trails of quartz and biotite inclusions. Data for such crystals are typified in fig. 3 where staurolite has formed along a narrow mica-rich band in a manner suggesting that the growth was restricted in the direction normal to the plane of the schistosity. For comparison two staurolites were analysed from Specimen D_3, one having grown in a thicker band where growth was not obviously restricted by the matrix in any direction (fig. 4*a*) and the other within a predominantly quartz-rich matrix (fig. 4*b*).

Staurolite formed within, or partly within, biotite pseudomorphs after regional garnet. Two examples from Specimen D_4 are illustrated, one showing the analysis of a staurolite occupying almost one-half of a pseudomorph (fig. 5*a*), and another one that has grown partly in a mica-rich band flowing around a biotite pseudomorph and partly within the pseudomorph (fig. 5*b*).

Staurolite formed around partially-replaced thermal garnets and almost completely replaced regional garnets. Fig 6*a* shows the analysis of a staurolite from Specimen D_2 that has partially enclosed a thermal garnet. In fig. 6*b* a similar compositional

relationship occurs when staurolite has grown entirely within a biotite pseudomorph and enclosed a remnant regional garnet.

Compositional variation across sector twin boundaries in staurolite. Nine staurolites were analysed, two of which are illustrated in fig. 7. All analysed elements at some stage show variation across the twin boundaries. Such variation may consist of an

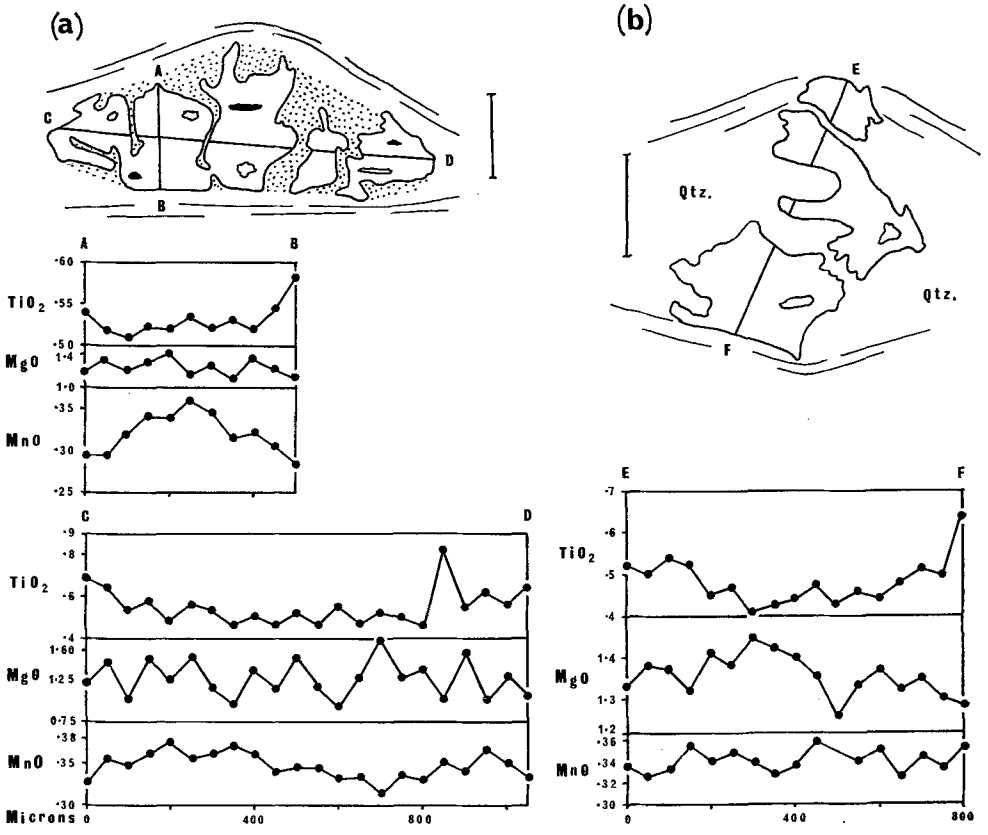

FIG. 4. Microprobe traces across staurolite formed in a wide mica-rich band (*a*), and staurolite from the same specimen but in a quartz-rich band (*b*). Dotted area in fig. 4*a* is sericite after staurolite. Scale bars are 400 μm.

obvious break, for example TiO_2 in fig. 7a, or a gradual increase or decrease towards the boundary.

To conclude, apart from the sector-twinned crystals, which will be discussed separately, all other analysed staurolite crystals show zoning characteristics, which can be summarized: Al_2O_3, Fe_2O_3 (analysed; total iron), and SiO_2 (by subtraction) are usually uniformly distributed across the crystals; in most cases TiO_2 increases towards the margins of the crystals (fig. 3 is an obvious exception); in most cases MnO is uniform and any variation is statistical, e.g. fig. 3 (however, some examples showing

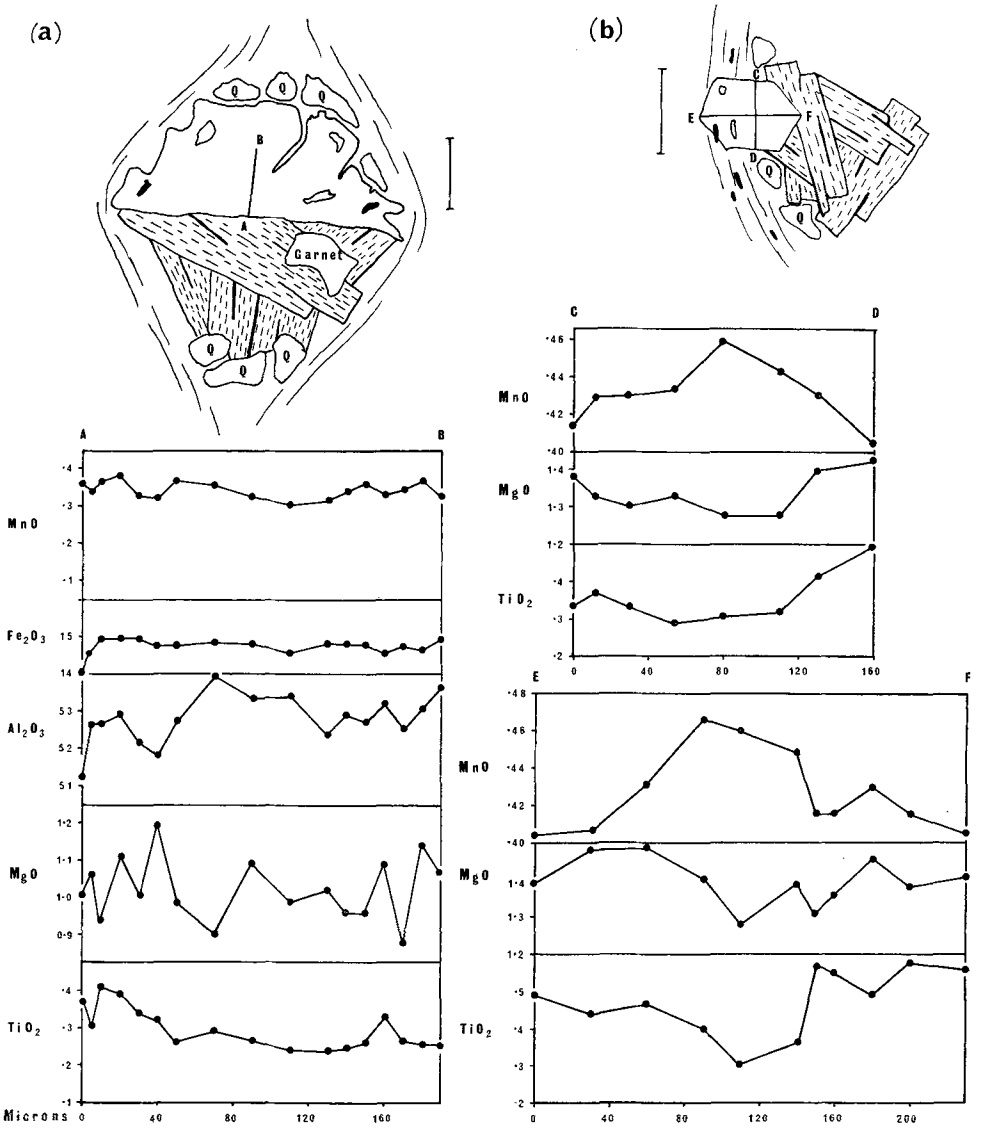

FIG. 5. Microprobe traces across staurolite totally within a biotite pseudomorph after regional garnet (*a*), and across a staurolite crystal partially within a similar pseudomorph (*b*). Stippled areas are biotite, black areas are ore, and quartz is denoted by Q. Clear inclusions within the staurolite are also of quartz. Scale bars are 200 μm.

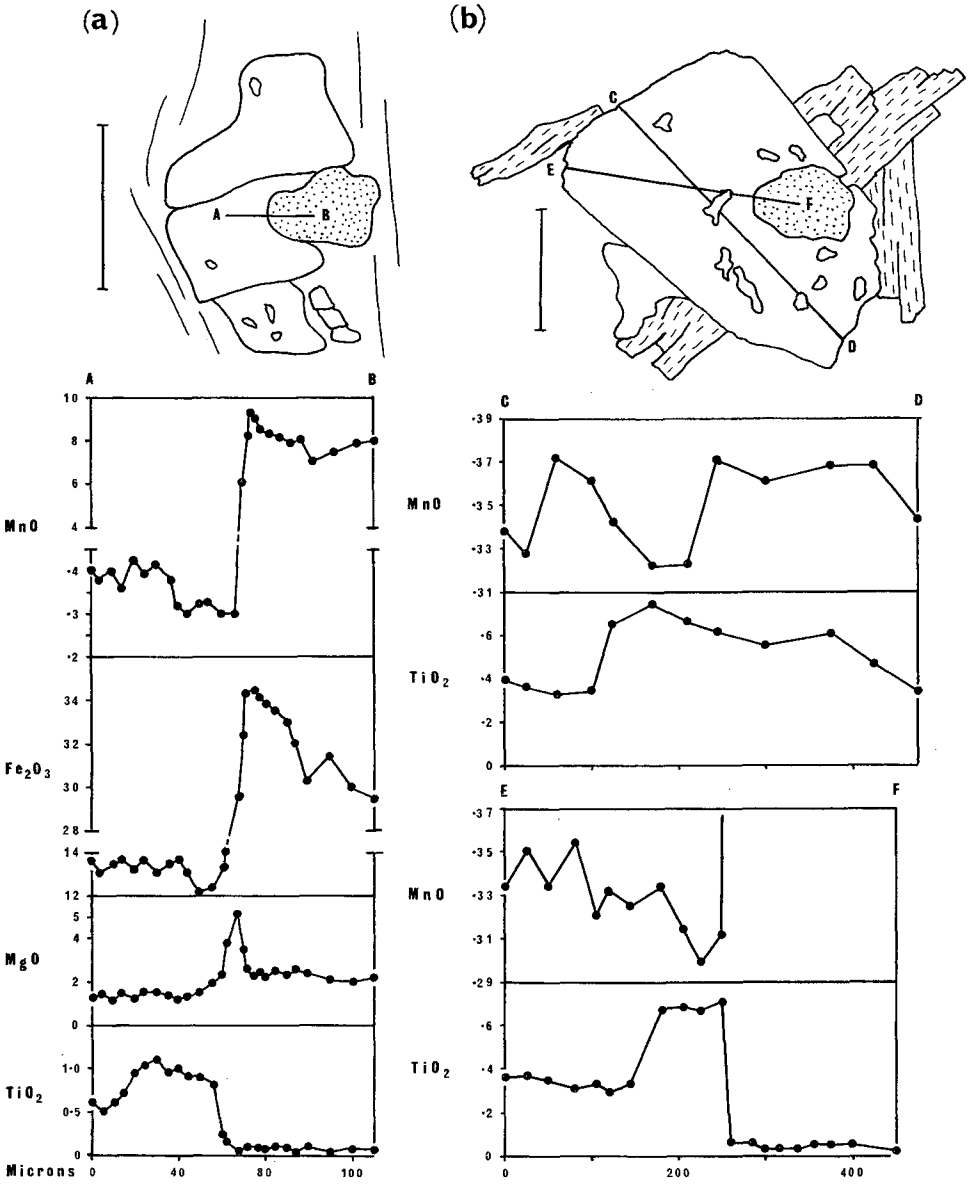

FIG. 6. Microprobe traces across staurolite–garnet grain boundaries caused by the envelopment of thermal garnet by staurolite (*a*), and regional garnet remnant by staurolite within a biotite pseudomorph after a regional garnet (*b*). Scale bars are 200 μm.

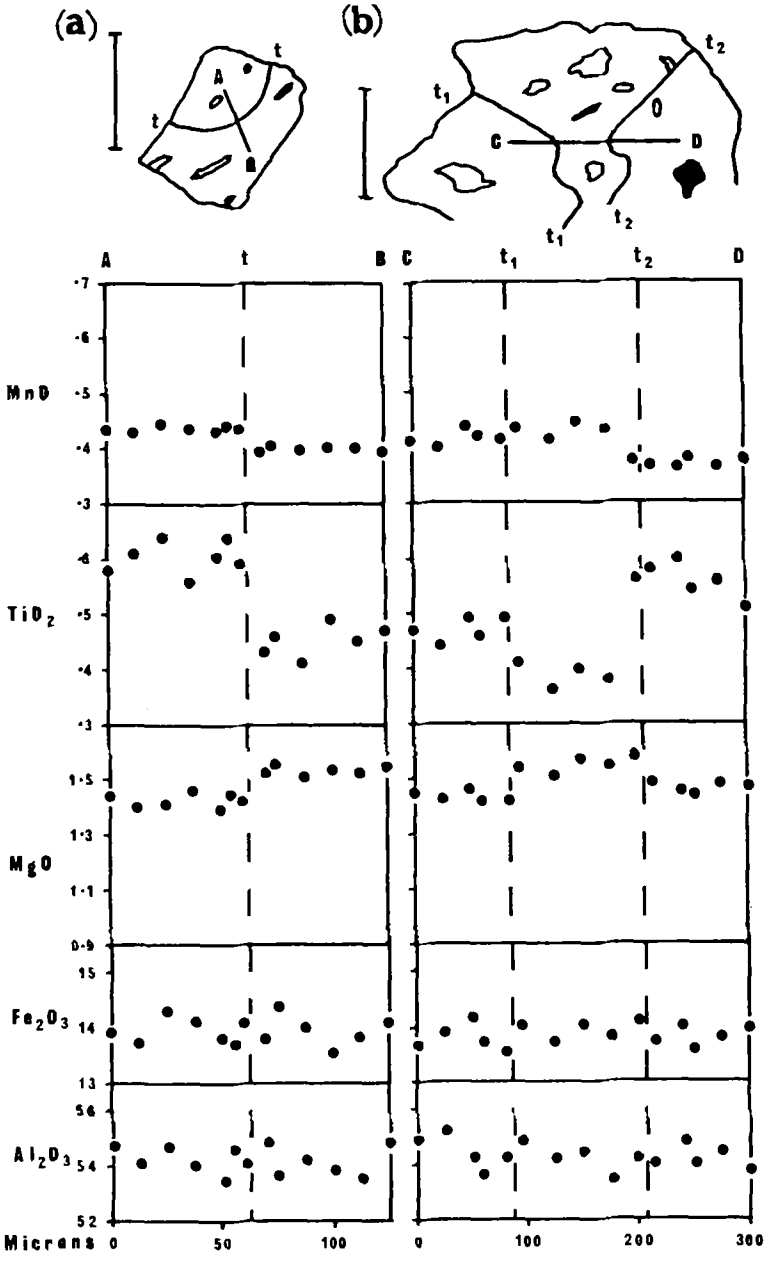

FIG. 7. Microprobe traces across sector twin boundaries in two staurolite crystals. Scale bars are 200 μm.

a small decrease at the margins also occur, e.g. fig. 5*b*); MgO is variable, sometimes sympathetic with TiO_2 (fig. 3) and sometimes antipathetic (fig. 4*b*).

Discussion

The only consistent trend appears to be shown by TiO_2. Even this, however, together with MnO and MgO, shows considerable variation depending on whether the growth of staurolite penetrates biotite pseudomorphs, encloses garnet fragments, or forms along narrow mica-rich bands bordered by quartz or a quartz-rich fabric.

The comparative irregularities of the compositional profiles when compared with those of the garnets from Ardara (Smellie, 1972 *b*), indicate that staurolite growth occurred under conditions of disequilibrium. Disequilibrium resulted during the increase in temperature, which accompanied emplacement, when the rate of staurolite growth became too rapid to maintain an equilibrium at the interface between the growing edge of the staurolite crystal and the diffusion or supply zone around the crystal. This in turn resulted in a limited or restricted diffusion of components to and from the interface, which meant that eventually the growing staurolite lattice had to accept whatever components were most readily available, provided they could be accommodated within the atomic lattice. The available components would depend on the sites of staurolite nucleation, for example, under such conditions of limited diffusion, a staurolite crystal within a biotite-rich matrix might be expected to accommodate more TiO_2 than from a matrix poor in biotite. Such a simple model could explain the asymmetry of the profiles and the inconsistency of the edge values described above.

Limited diffusion on a local scale is well exemplified in figs. 6*a* and *b*, in which staurolite has enclosed a thermal garnet and a regional remnant garnet. It is clear from comparison of these and other garnet–staurolite interfaces (Smellie, 1972 *b*) that no obvious interaction between staurolite and garnet has occurred; all indications are that the garnet alteration to biotite had been initiated before being completely enclosed by the staurolite. Such alteration meant that both regional and thermal varieties of garnet were surrounded, or partly surrounded, by biotite resulting from the garnet breakdown (fig. 2*a*). It appears reasonable, therefore, to conclude that staurolite has grown partly from this biotite, as it eventually enclosed the garnet. One obvious feature in the figures is a zone of high TiO_2 and low MnO concentration bordering the garnets. As the TiO_2 content of biotite is high (approx. 1·4 %) compared with that of average staurolite values (approx. 0·4 %), there will tend to be an excess of TiO_2 as staurolite forms from the biotite. This excess will continually be rejected as staurolite growth approaches the garnet boundary, a process somewhat analogous to zone refining, until a stage is reached when restricted diffusion prevents the TiO_2 from moving away from the staurolite, and it is forced to accommodate additional TiO_2 as it finally encloses the garnet. MnO decreases antipathetically because biotite (approx. 0·15 % MnO) contains less MnO than staurolite (approx. 0·50 %) so that as staurolite growth continues, the MnO supply from biotite becomes increasingly inadequate to maintain a uniform MnO content in the staurolite. The result is a gradual decrease of MnO towards the garnet. According to this hypothesis

MgO might be expected to show a similar trend to TiO_2. The MgO distribution in fig. 6*a* shows a sharp peak at the interface. This indicates that MgO, in contrast to TiO_2, is not readily accommodated within the atomic lattice of staurolite and has therefore become trapped because of limited diffusion away from the growing staurolite.

The compositional profiles in fig. 4*b* (traverse EF), may also be partly explained in a similar manner. The part of the staurolite that has grown into the biotite pseudomorph shows a similar antipathetic TiO_2–MnO relationship. It is possible, therefore, that as the staurolite grew into the pseudomorph diffusion was inadequate to disperse the excess TiO_2 and supply the necessary MnO needed to maintain compositional uniformity across the staurolite.

Slight compositional differences occur across twin boundaries. The significance of these variations is difficult to evaluate because no universal stage work was carried out to identify the crystallographic faces under investigation. All of the elements show some variation, the most commonly variable components being TiO_2, MnO, and MgO.

Sector compositional variations and zoning have been described by Hollister and Bence (1967) and Hollister (1970). Hollister and Bence had the advantage of a large idiomorphic crystal from which several orientated sections were cut and analysed. They found that staurolite possessed three sectors, each with a distinctive content of Al, Si, Ti, Fe, Mg, and Mn. Hollister (op. cit.) proposed a model that might well apply to Ardara, but the variation of edge values in the latter case suggest that during the final stages of staurolite growth disequilibrium occurs between the growing surface layers of the staurolite and the matrix, in addition to the disequilibrium between the bulk of each sector and the matrix.

Conclusions

The major components are, in general, regularly distributed within the Ardara staurolites. The main variations are caused by minor components such as TiO_2, MgO, and MnO. The distribution of these seem to depend on two main factors: compositional irregularities that reflect the variation of the matrix in which the staurolite is growing, thus implying restricted diffusion on a localized scale; and rapid growth conditions associated with contact metamorphism.

Acknowledgements. I am especially indebted to Dr. K. A. Jones (Belfast) for many stimulating discussions and his helpful criticism, which improved the manuscript. Thanks are due to Dr. R. B. Elliott and Mr. C. C. Ferguson (Nottingham) for their critical reading of the manuscript and Mr. D. Jones for photography.

This paper forms part of a major study carried out during the tenure of a Postgraduate Studentship from the Ministry of Education, Northern Ireland, which is gratefully acknowledged.

REFERENCES

AKAAD (M. K.), 1956*a*. *Quart. Journ. Geol. Soc.* **112**, 263–88.

—— 1956*b*. *Geol. Mag.* **93**, 377–92.

ATHERTON (M. P.), 1965. *Controls of metamorphism* (eds. PITCHER, W. S., and FLINN, G. W.), Oliver and Boyd (Edinburgh and London), 169–202.

ELLITSGAARD-RASMUSSEN (K.), 1954. *Medd. Grønland*, 136.
HOLLISTER (L. S.) and BENCE (A. E.), 1967. *Science*, **158**, 1053–6.
—— 1970. *Amer. Min.* **55**, 742–66.
JUURINEN (A.), 1956. *Ann. Acad. Sci. Fen. Ser. A*, Sec. 3, 47.
NAGGAR (M. H.) and ATHERTON (M. P.), 1970. *Journ. Petrol.* **11**, 549–89.
PITCHER (W. S.) and SINHA (R. C.), 1958. *Quart. Journ. Geol. Soc.* **113**, 393–408.
—— and READ (H. H.), 1963. *Journ. Geol.* **71**, 261–96.
SMELLIE (J. A. T.), 1972 *a*. *Min. Mag.* **38**, 614–17.
—— 1972 *b*. Unpubl. Ph.D. thesis, Queen's University, Belfast.
WILLIAMSON (D. H.), 1953. *Geol. Mag.* **90**, 353–61.

[*Manuscript received 13 August 1973; revised 13 December 1973*]